

Durham Research Online

Deposited in DRO:

11 April 2016

Version of attached file:

Accepted Version

Peer-review status of attached file:

Peer-reviewed

Citation for published item:

Stricker, S and Jones, S.J. and Grant, N. (2016) 'Importance of vertical effective stress for reservoir quality in the Skagerrak Formation, Central Graben, North Sea.', *Marine and petroleum geology.*, 78 . pp. 895-909.

Further information on publisher's website:

<http://dx.doi.org/10.1016/j.marpetgeo.2016.03.001>

Publisher's copyright statement:

© 2016 This manuscript version is made available under the CC-BY-NC-ND 4.0 license
<http://creativecommons.org/licenses/by-nc-nd/4.0/>

Additional information:

Use policy

The full-text may be used and/or reproduced, and given to third parties in any format or medium, without prior permission or charge, for personal research or study, educational, or not-for-profit purposes provided that:

- a full bibliographic reference is made to the original source
- a [link](#) is made to the metadata record in DRO
- the full-text is not changed in any way

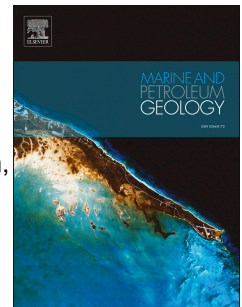
The full-text must not be sold in any format or medium without the formal permission of the copyright holders.

Please consult the [full DRO policy](#) for further details.

Accepted Manuscript

Importance of vertical effective stress for reservoir quality in the Skagerrak Formation,
Central Graben, North Sea

Stephan Stricker, Stuart J. Jones, Neil T. Grant



PII: S0264-8172(16)30058-7

DOI: [10.1016/j.marpetgeo.2016.03.001](https://doi.org/10.1016/j.marpetgeo.2016.03.001)

Reference: JMPG 2488

To appear in: *Marine and Petroleum Geology*

Received Date: 13 January 2016

Accepted Date: 1 March 2016

Please cite this article as: Stricker, S., Jones, S.J., Grant, N.T., Importance of vertical effective stress for reservoir quality in the Skagerrak Formation, Central Graben, North Sea, *Marine and Petroleum Geology* (2016), doi: 10.1016/j.marpetgeo.2016.03.001.

This is a PDF file of an unedited manuscript that has been accepted for publication. As a service to our customers we are providing this early version of the manuscript. The manuscript will undergo copyediting, typesetting, and review of the resulting proof before it is published in its final form. Please note that during the production process errors may be discovered which could affect the content, and all legal disclaimers that apply to the journal pertain.

Importance of vertical effective stress for reservoir quality in the Skagerrak Formation, Central Graben, North Sea.

Stephan Stricker^a, Stuart J. Jones^a, Neil T. Grant^b

^a*Department of Earth Sciences, Durham University, South Road, Durham, DH1 3LE, UK*

^b*ConocoPhillips UK Ltd., Rubislaw House, North Anderson Drive, Aberdeen, AB156FZ, UK*

Abstract

The complex fluvial sandstones of the Triassic Skagerrak Formation of the Central Graben area, North Sea, provide a number of prolific high-pressure high-temperature (HPHT) hydrocarbon reservoirs. The reservoir sandstones comprise fine to medium-grained sub-arkosic to arkosic sandstones that have experienced broadly similar burial and diagenetic histories to their present-day maximum burial depth. Despite similar diagenetic histories the fluvial reservoirs show major variations in reservoir quality and preserved porosity. Reservoir quality varies from excellent with anomalously high porosities of up to 35% at burial depth of >3500 metre below sea floor (m bsf) to non-economic with porosities <10% at burial depth of 4300 m bsf.

This study has combined detailed petrographic analyses, core analysis and pressure history modeling to assess the impact of differing vertical effective stresses (VES) and high pore fluid pressures (up to 80 MPa) on reservoir quality. It has been recognized that fluvial channel sandstones of the Skagerrak Formation in the UK sector have experienced significantly less mechanical compaction (under-compacted) than their equivalents in the Norwegian sector. This has had a significant impact upon reservoir quality, even though the presence of chlorite grain coatings inhibited macroquartz cement overgrowths across all Skagerrak Formation reservoirs. The onset of overpressure started once the overlying chalk seal was buried deeply enough to form a permeability barrier to fluid escape. It is the accrual rate of overpressure and its effect on the VES history that is key to determining the reservoir quality of these channelised sandstone units. The results are consistent with a model where vertical effective stress affects both the compaction state and subsequent quartz cementation of the reservoirs.

Introduction

The reservoir quality of deeply buried sandstones is the combined product of depositional processes and subsequent diagenesis during progressive burial. Deposition controls the composition of the sand, including its grain size distribution which has an over-arching influence in determining reservoir properties. Relative differences between sandstone facies in terms of porosity and permeability are preserved during burial, so facies is a key factor in controlling reservoir performance. Burial-related diagenesis also has an important role to play as it can destroy, preserve, or enhance the reservoir quality, whatever the facies. High porosities in deeply buried siliciclastic reservoirs are exceptional and have commonly resulted from diagenetic cementation followed by dissolution (e.g. Bloch et al., 2002; Taylor et al., 2010). The role played by vertical effective stress (VES) during initial mechanical and chemical compaction processes is generally considered to be less significant. Primary porosity is reduced by mechanical compaction processes at shallow depths, where grain rearrangement (frictional slippage, rotation and sliding), deformation of soft grains (e.g. lithic fragments), and fracturing of ridged grains (e.g. quartz and feldspar), can occur. At the higher temperatures and pressures of deep burial, chemical compaction takes over and includes mineral growth and inter-granular pressure solution (e.g. Houseknecht, 1987; Chuhan et al., 2002; Paxton et al., 2002). Mechanical and chemical compaction processes are irreversible and eliminate inter-granular volume (IGV) that would otherwise remain fluid-filled or become occupied by cements that might dissolve during later diagenesis (Houseknecht, 1987). Thus inhibition of compaction is vital for porosity maintenance to depth.

Two processes are known to inhibit sediment compaction: cement precipitation that strengthens the grain framework and the development of pore fluid overpressure. Stabilization of the framework and enlargement of the grain contact areas can be achieved by the precipitation of small quantities of cement, such as carbonate, halite or quartz, and the porosity preservation is strongest if precipitation occurs at shallow depth. Fluid

overpressure supports the grain framework and reduces the effective stress acting on the framework. Both processes can significantly reduce mechanical and chemical compaction. Pore fluid pressures in sedimentary basins remain hydrostatic during burial where the rocks can drain freely. Overpressure occurs where the fluid cannot drain rapidly enough for the pore pressure to remain hydrostatic as the bulk rock volume is reduced by compaction processes. Low permeability retards fluid flow and so overpressures develop preferentially where rocks are sealed by thick successions of fine-grained sediment. Fluid volume expansion due to cracking of oil to gas, transformation of smectite to illite, lateral transfer, and temperature increase can also lead to the development of excess pore pressure (e.g. (Osborne and Swarbrick, 1997; Swarbrick and Osborne, 1998; Swarbrick et al., 2002). The overpressure supports the grain framework and decreases the stress acting on the grain contacts which leads to lower normal effective stresses (Terzaghi's effective stress concept).

The aim of this paper is to investigate the reason for the porosity variations in the Skagerrak Formation in the Central North Sea and how anomalously high porosities have been preserved even though it is deeply buried and at high temperatures. One-dimensional pore pressure and burial history models are combined with detailed petrography to assess the role played by overpressure on VES and reservoir quality. Analysis of the key processes responsible for this porosity preservation requires depositional effects to be taken into account. This has been done by careful focus on reservoir facies with similar grain size and sorting. The results can be used to help predict reservoir quality in undrilled structures.

Geological setting

The Central Graben of the North Sea is approximately 550 km long with a width of 70-130 km and is part of a NW-SE trending extension of a trilete rift system, with the Viking Graben as the northern arm and the Inner and Outer Moray Firth as the western arm. The North Sea Central Graben is divided into the East and the West Central Graben by the Forties-Montrose and the Josephine Ridge medial horst blocks, and separates the Norwegian platform in the east from the UK continental shelf in the west (Figure 1). The complex rift

system developed in at least two major extensional phases, one in the Permian-Triassic (290-210 Ma) and another in the Late Jurassic (155-140 Ma) (Gowers and Sæbøe, 1985; Glennie, 1998). The geological history has commonly been divided into pre-rift, syn-rift and post-rift phases. The syn-rift sediments are mainly siliciclastic Triassic and Jurassic sediments with a cumulative thickness of 1000-4000 m. The post-rift sediments comprise the Cretaceous to Holocene successions, of up to 4500 m in total thickness, which are dominated by shale, sandstone, silty-sandstone and thick Upper Cretaceous chalk units including the Ekofisk, Tor and Hod Formations (Figure 2) (Goldsmith et al., 2003). These highly cemented and compacted chalk units provide the main seal for the highly overpressured sub-Chalk reservoirs in the Central Graben, North Sea (Mallon and Swarbrick, 2002, 2008; Swarbrick et al., 2010). The focus area for this study includes the Heron (well 22/29-5RES1) and Skua (well 22/24b-7) fields from the Heron Cluster in UK quadrant 22, the Jade (well 30/2c-4) and Judy (wells 30/7a-7, -8, -9, 11Z, -P3 & 30/13-5) fields from the Josephine Ridge in UK quadrant 30, and the Cod (well 7/11-7) and Gaupe (well 6/3-1) fields in Norwegian quadrants 7 and 6, respectively (Figure 1). This broad areal coverage allows a regional perspective on the post-depositional processes that have influenced porosity preservation in the Skagerrak Formation.

Triassic Skagerrak Stratigraphy

The Triassic strata of the Central North Sea area are dominated by thick alluvial successions deposited in a closed or internally draining basin with no apparent connection to a marine realm (Goldsmith et al., 2003). The general Triassic succession is subdivided into the Early Triassic Smith Bank Formation (shales, evaporites and thin sands) and the Middle to Late Triassic Skagerrak Formation (a thick sequence of interbedded sands and shales) (Figure 2). The Middle to Late Triassic Skagerrak Formation comprises 500-1000 m of predominantly continental braided and meandering fluvial deposits, terminal fluvial fans and lacustrine shale (McKie and Audretsch, 2005; De Jong et al., 2006; Kape et al., 2010). The stratigraphic nomenclature of the Triassic for the Central Graben was defined by Goldsmith

et al. (1995, 2003), based on detailed biostratigraphic and lithostratigraphic correlation of wells from the Josephine Ridge. This nomenclature has been extended and correlated towards the Forties-Montrose High area by McKie and Audretsch (2005). The Skagerrak Formation can locally be subdivided into two sand-dominated members (Judy and Joanne) and two mud-dominated members (Julius and Jonathan) for UK quadrants 22 and 30, but is not subdivided in Norwegian quadrants 6 and 7 (Goldsmith et al., 2003). The sand-dominated units include sheetflood deposits and multi-storey stacked channel sandbodies (Goldsmith et al., 1995; McKie and Audretsch, 2005), whereas the mud-dominated units include basin-wide floodplain, lacustrine shale, loess and playa deposits. The thick and laterally extensive mud-dominated units provide the main correlative units for the Skagerrak Formation in the Central Graben (McKie and Audretsch, 2005). The Triassic stratigraphy is incompletely preserved due to deep erosion during the Middle and Late Jurassic (Figure 2) (Erratt et al., 1999).

The Triassic Smith Bank and Skagerrak sediments accumulated directly on top of the thick Late Permian Zechstein salt in a series of salt-controlled and fault-controlled minibasins or pods. The Late Permian Zechstein salt strongly controlled the deposition by forming withdrawal basins due to a combination of localised loading and structural extension (Smith et al., 1993; Bishop, 1996; Matthews et al., 2007) within an overall rift setting. The predominantly fine grained Smith Bank Formation represents the basal part of the pod infill, and was deposited in lacustrine and playa settings within confined minibasins. These enlarged and amalgamated during deposition of the overlying Skagerrak Formation as salt budgets waned and diapirism became localised rather than the salt continued to form extensive salt walls. Pod development was active throughout the Triassic and is mainly responsible for the preservation of Middle to Late Triassic Skagerrak Formation in the study area. Where the Late Permian salt was thickly developed, it prevented grounding of the pods on the underlying Rotliegend basement. Salt withdrawal has allowed considerable thicknesses of Skagerrak sediment to accumulate within pods as well as being responsible for great variation in thickness both within and between pods. The consequent facies

variability has influenced sandstone reservoir thickness and subsequent diagenetic cementation (Nguyen et al., 2013).

Methodology

Sampling

Core samples and the thin sections examined in this study are from Triassic Skagerrak sandstones in the four fields in the UK sector: Heron (well 22/29-5RES1; 136 samples), Skua (well 22/24b-7; 32 samples), Jade (well 30/2c-4; 20 samples), and Judy (wells 30/7a-7, -8, -9, -11Z, -P3 & 30/13-5; 85 samples in total) and from two fields in the Norwegian sector: Cod (7/11-7; 39 samples) and Gaupe (6/3-1; 90 samples). The samples were selected from channel sands, the sedimentary facies in the available core material that is expected to have the best reservoir properties because of good sorting and an absence of matrix.

Petrography

Thin sections of core samples were used to measure optical porosity, grain size, composition and inter-granular volume. Optical porosity was measured by the digital image analysis technique jPOR (Grove and Jerram, 2011) on blue epoxy-impregnated thin sections. Uncorrected helium porosity measurements, making use of Boyle's law on core samples, were taken from core analysis reports. Grain size distribution was determined from analysis of thin section micrographs with the Leica QWin (V. 3.5.0) software. Sandstone composition was measured by point counting, with 300 counts per thin section using a standard petrographic microscope. Further petrographic analysis, such as intergranular-volume (IGV), total cement volume (C) and grain contact analysis, were exclusively performed on fine-grained samples with similar sorting. Inter-granular volume and total cement volume were measured by point counting with 300 counts per thin section using a standard petrographic microscope. Grain-to-grain contacts were counted and classified by counting a line of 50 grain contacts per thin section.

One-dimensional basin modelling

Pore pressure in the Skagerrak sandstones for all six fields was modelled in one dimension using Schlumberger's PetroMod (V. 2012.2) software. This one-dimensional modelling provides a good insight into overpressure build-up by disequilibrium compaction and pore fluid expansion due to increasing temperature. However, the models do not include other mechanisms for generating excess pore pressure such as fluid flow or hydrocarbon cracking, and are only able to take vertical stress into account. Any influence of clay mineral diagenesis on fluid pressure development is ignored. PetroMod is based on a forward modelling approach to calculate the geological evolution of a basin from the burial history. The burial history and lithology are inferred from the present-day well stratigraphy, well log lithology and lithological description of the modelled units (Tables 1 & 2). We used the thermal upwelling basement palaeo-heat flow model of (Allen and Allen, 1990) with 63–110 mW/m² (average of 80 mW/m²) during syn-rift phases and 37–66 mW/m² (average 50 mW/m²) during post-rift phases combined with the palaeo-surface temperature history published by Swarbrick et al., 2000. The burial history models are calibrated against present-day RFT temperature measurements, corrected after Andrews-Speed et al. (1984), measured Triassic sandstone porosities (Boyle's law) and carefully adjusted towards present-day formation pressure measurements by considering late stage, high temperature overpressure mechanisms (Osborne and Swarbrick, 1997; Isaksen, 2004). The lithological unit types used in these models are mainly PetroMod (V. 2012.2) default lithology types, based on well log descriptions and core analysis reports for the investigated wells. Exceptions are the Hod lithology type present in the UK models and the lithology type of the Skagerrak sandstone members. The Hod chalk unit is modified to represent the North Sea non-reservoir chalk (Table 3) and match the compaction trend and permeability trend given by (Mallon and Swarbrick, 2002, 2008). The North Sea non-reservoir chalk is a laterally extensive low-permeability rock unit that represents the major vertical fluid flow barrier in the Central North Sea (Mallon and Swarbrick, 2008). The Triassic Skagerrak sandstone of the Joanne and Judy Sandstone Members is simulated by a mixture of PetroMod (V. 2012.2)

default lithologies (80% sand, 10% silt, 10% shale) combined with a regional compaction trend for shaly sandstone given by (Sclater and Christie, 1980).

Results

Grain size, composition and porosity distribution

The 347 investigated samples from the Heron Cluster fields (Heron – 136 and Skua – 32), the J-Ridge fields (Jade – 20 and Judy – 85), and the Norwegian fields (Cod – 30) and Gaupe – 90) vary compositionally within a narrow range of arkosic and lithic-arkosic sandstones. The grain size of the samples varies between silt and coarse-grained sand, with small regional differences (Figure 3). The sample sets show a wide range of optical porosities from below 1% up to 35% (Figures 3 & 4) with higher maximum porosities occurring at coarser grain sizes (Figure 3 & Table 4). The optical porosity data sets have been complemented by additional helium core plug porosity data, measured using Boyle's law (uncorrected for possible decompaction effects). The helium core plug porosities measure the total porosity and are mostly greater than the optical measured porosity values (Figure 4 & Table 4), indicating the presence of significant microporosity within the sandstones. This is likely to reside with the clay cements and matrix, within partially dissolved grains and as small voids along grain boundaries.

Intergranular volume and porosity loss

Intergranular volume (IGV), or minus-cement porosity, is the sum of intergranular pore space, intergranular cement and depositional matrix (Houseknecht, 1987, 1988; Paxton et al., 2002). IGV is an excellent indicator for the degree of mechanical compaction of clastic sediments due to its dependence on vertical effective stress (VES) and its diminishing trend with ongoing compaction. Nevertheless, IGV can also be influenced by factors such as early cementation (grain framework strengthening or locally pore filling) or early pore fluid overpressure.

The IGV values of the six sample sets show both wide internal variations and variations between the different sample sets (Table 5). IGV averages of the shallower buried sample sets (e.g., from the Judy and Skua fields) are generally higher than those of the deeper sample sets (e.g., Cod and Jade). This difference points to variations in compaction state between fields. Mechanical compaction of a fine-medium grained, well sorted sand, typical of the Skagerrak channel facies, should be able to reduce IGV from a starting point around 45% at deposition (e.g. Bears and Weyl, 1973) to around 26% when tightly packed grain framework established (e.g. Paxton et al., 2002). The grain composition will influence the amount of compaction with feldspars more likely to fracture and deform than quartz grains. Early framework stabilising cements or overpressure development help retard compaction during burial.

The total cement volume has been measured and can be used in combination with the IGV to calculate the porosity loss by compaction (COPL) and by cementation (CEPL) using the following equations by (Lundegard, 1992):

$$COPL = P_i - \left(\frac{(100 - P_i)P_{mc}}{100 - P_{mc}} \right) \quad (1)$$

$$CEPL = (P_i - COPL) \left(\frac{C}{P_{mc}} \right) \quad (2)$$

where P_i is the initial or depositional porosity and P_{mc} is the intergranular volume or minus-cement porosity calculated from by subtracting the total cement volume, C , from the total optical primary porosity, P_o . The calculated COPL and CEPL are accurate if three conditions are met. First, the assumed initial porosity P_i is correct. Second, the amount of cement derived by local grain dissolution is negligible or known. And third, the amount of framework mass exported by grain dissolution is negligible or known (Lundegard, 1992). The initial or depositional porosity for the Triassic Skagerrak sandstones samples is assumed to have been 45% (Bears and Weyl, 1973; Houseknecht, 1987; Lundegard, 1992; Chuhan et al.,

2002; Paxton et al., 2002). The COPL-CEPL results (Figure 5) indicate mechanical and chemical compaction as the main drives for porosity loss of the Heron, Skua, Jade, Judy and Cod sample sets, whereas the COPL-CEPL results of the Gaupe sample set indicate a more mixed porosity loss, albeit with a stronger tendency towards compaction.

Compaction indicators

Evidence for both mechanical and chemical compaction can be observed in the investigated fine grained sandstone samples. Mechanical compaction is recorded by features such as grain rearrangement, grain deformation, denser grain packing, and the frequency of distinctive grain contacts, such as point and long/tangential grain contacts for low mechanical compaction or concavo-convex and sutured grain contacts for high mechanical compaction (Table 6). Chemical compaction of quartz-rich sandstones occurs by pressure solution at grain contacts and is indicated by the presence of concavo-convex and/or sutured grain contacts.

The Judy sample set displays a low grain-packing density, often with apparently 'floating' grains, i.e., grains surrounded by pores in two-dimensional space (Figure 6A), and a high number of point contacts between the grains (Table 6). These features are characteristic of a relatively low compaction state or under-compaction in relation to similar hydrostatically pressured sandstones at equivalent burial depth (porosity-depth relationship for hydrostatically pressured shaly sandstone by Sclater and Christie (1980)). 'Floating' grains are not observed in the Heron Field sample set which has a slightly denser grain packing, a lower number of point contacts and slight bending of mica grains, but still has a low compaction state. The Jade and Skua sample sets generally show more mechanical compaction with denser grain arrangements and bent mica grains, and more features characteristic of chemical compaction, such as a higher frequency of concavo-convex contacts than the Heron and Judy field samples (Table 6 & Figure 6B). The Gaupe and Cod samples have a high grain-packing density and a high number of grain to grain contacts per grain (Figure 6C). These characteristics indicate a high degree of mechanical compaction,

also recorded by the high frequency of soft grain deformation, such as bent micas (Figure 6D) and deformed lithic fragments. Chemical compaction is very common in the Norwegian data sets with petrographic evidence such as concavo-convex and sutured grain contacts in both the Gaupe and, especially, the Cod samples (Figure 6E & F). The grain framework of the Cod samples is dominated by concavo-convex grain contacts and shows the highest frequency of sutured grain contacts. Evidence of strong chemical compaction, i.e., sutured grain contacts, is rarely observed in the Jade and Skua samples, and are completely absent in the Judy and Heron field samples (Table 6).

One-dimensional basin modelling

The one-dimensional models show the evolution of burial depth, pore fluid overpressure and VES throughout the geological history for the top of the Triassic Skagerrak reservoir formation in the investigated fields/wells. Each model was set up from the present-day well stratigraphy, well log lithology and lithological description (Tables 1 & 2) and carefully calibrated against measured Skagerrak sandstone porosities (Figure 4). This was achieved by using observed and published rock properties for key horizons, as described above. Furthermore, each model was calibrated against corrected RFT temperatures and carefully adjusted towards measured present-day formation pressures by considering late stage, high temperature overpressure mechanisms (Osborne and Swarbrick, 1997; Swarbrick and Osborne, 1998; Isaksen, 2004). The burial history of the Skagerrak Formation can generally be subdivided into two main burial phases. The first episode of burial occurred at a relatively slow rate from the time of deposition (220 Ma) to 100-70 Ma. Because all the hydrocarbon fields studied are located on structural highs, the impact of Late Jurassic rift-related subsidence is largely absent from the burial history plots, or is obscured by erosion associated with the Base Cretaceous (end-rift) unconformity. The second phase of burial is related to post-rift subsidence and infilling of accommodation space within the Central Graben from 90 Ma until the present-day. The fields now all reside at maximum burial depth.

The burial histories of the Heron Cluster fields, the J-Ridge fields and the Norwegian fields show similar burial histories due to their proximity to each other (Figure 1).

The Judy Sandstone Member in the Heron and Skua fields experienced a phase of burial with maximum depths of around 1200 m followed by a phase of uplift during the early burial history (deposition to 165 Ma). Burial depth remained shallow, with maximum depths of around 500 m from 165 Ma until 90 Ma. From 90 Ma onwards, burial was rapid and the Triassic sandstone members are at their maximum burial depths at the present day (Figure 7). The calculated overpressure started to build up in the Judy Sandstone Member at the Heron and Skua fields at around 60 Ma and 45 Ma, respectively, with onset burial depths of around 1550 m and 1250 m for the reservoir formation tops, respectively. The development of this overpressure reflects disequilibrium compaction beneath the overlying Chalk. Overpressure increased continuously with ongoing burial and reached 1 MPa at burial depths of 1650 m and 1750 m in the Heron and Skua fields. Pore pressures are at their maxima at the present day, around 41 MPa for the Heron field and 28 MPa for the Skua field. The continuous overpressure increase from its onset around 60 Ma has reduced the rate of VES accrual. The maximum modelled VES is reached around 10 Ma, with a value of approximately 21.5 MPa in the Heron Field and 23 MPa in the Skua Field. This was followed by a trend of decreasing VES until the present day due to significant overpressure build-up in the last 10 Myr. The present-day VES values for the two fields are around 6 MPa for Heron and 12 MPa for Skua (Figure 7).

The Joanne Sandstone Member of the J-Ridge Jade and Judy fields was also shallowly buried until 90 Ma. This early history commenced with a short phase of shallow burial followed by uplift during the latest Triassic and early Jurassic. Rapid burial commenced around 90 Ma and continued almost without interruption again towards the present-day maximum burial depth (Figure 7). The 1D models suggest pore fluid overpressure started to build up from around 65 Ma and 50 Ma when burial was around 1250 m and 1350 m for the Jade and Judy fields, respectively. The modelled overpressure in both Triassic formations increased with ongoing burial and reached 1 MPa in Jade and Judy

at burial depths of around 1400 m and 1500 m, respectively. Pore fluid overpressures are at their maxima at the present day with values around 38 MPa and 25 MPa in the Jade and Judy fields respectively. As before, the continuous increase of overpressure reduced the rate of VES accrual in both reservoirs (Figure 7). Prior to production, the estimated VES was 11 MPa in the Jade Field and 8 MPa in the Judy Field when buoyancy of the trapped hydrocarbon columns is included. Without these columns, the VES related to aquifer overpressure (modelled by 1D PetroMod) was around 17 MPa and 16 MPa, respectively. Maximum VES of the J-Ridge fields was again reached at around 10 Ma followed by VES reductions until the present day by additional overpressure mechanisms. Maximum VES in the Jade and Judy fields is modelled as 22 MPa and 19.5 MPa, respectively, at approximately 10 Ma (Figure 7).

The Triassic sandstones of the Norwegian Cod and Gaupe fields also experienced a shallow burial phase from deposition to around 140 Ma and 60 Ma, followed by a phase of continuous burial towards present-day maximum depths (Figure 7). Modelled overpressure in the reservoir sandstones started to build up during the continuous burial at depths of around 1350 m and 1150 m. The overpressure increased during ongoing burial and reached 1 MPa at 50 Ma (~2200 m) and 20 Ma (~2300 m) in the Cod and the Gaupe fields, respectively. Overpressure in the Cod field increased significantly from the Late Miocene to the present-day overpressure of 34 MPa. Overpressuring of the Triassic reservoir sandstones led to a VES reduction from around a maximum modelled value of 36 MPa to 19 MPa at the present day (Figure 7). The VES history of the Gaupe field is less affected by overpressure due to its late onset and low magnitude. Present-day overpressure in the Gaupe Field is modelled as 6.5 MPa, with a VES of around 27 MPa for the Gaupe sandstones (Figure 7).

Discussion

Implications of overpressure on vertical effective stress

VES is long recognised as the main driver of early porosity loss by mechanical compaction processes during shallow burial (0–2500 m) (Houseknecht, 1987, 1988; Paxton et al., 2002). Limiting the accrual rate or reducing the VES during burial by pore fluid overpressure can slow down or arrest mechanical compaction and reduce its effect on porosity loss, leading to the maintenance of primary porosity to depth (Bloch et al., 2002; Nguyen et al., 2013; Stricker and Jones, 2016). Even though this effect has been well known since Terzaghi's introduction of the effective stress concept, the impact of low VES due to overpressure has often been overlooked or underestimated in reservoir quality studies (e.g. Taylor et al., 2015). However, to preserve enhanced reservoir quality by overpressure, the magnitude of overpressure, its continued maintenance during progressive burial, and the depth where the overpressures first started to develop must all be considered. Late development of overpressure at greater depth (for example by fluid transfer or expansion) will not be associated with a reduced compaction state and enhanced porosity.

IGV as a proxy for maximum VES and shallow overpressure development

As discussed by (Houseknecht, 1987, 1988; Lundegard, 1992; Ehrenberg, 1995; Paxton et al., 2002), IGV, or minus-cement porosity, with its diminishing trend with ongoing burial depth or increased VES reflects the degree of mechanical compaction (e.g. grain rearrangement) and chemical compaction at greater depths (i.e. pressure solution).

The quantification of the IGV development with depth has been the subject of various studies (e.g. Houseknecht, 1987, 1988; Lundegard, 1992) which highlighted significant IGV loss by mechanical compaction during shallow burial, with a physical lower limit of 26-30% established at burial depth of 2000-2500 m, depending on the grain size, sorting and rock composition. A global study by (Paxton et al., 2002) resulted in an intergranular volume compaction curve with depth, which identified major IGV loss (10-12%) during shallow burial (<1500 m) in uncemented, rigid-grained sandstones and established a physical lower limit of around 26% at 2500 m burial depth. Therefore IGV values of less than 26% reflect

significant chemical compaction (i.e. pressure solution) within the rigid grain frame work (Paxton et al., 2002).

The application of the physical lower limit by Paxton et al. (2002) on the average IGV of the six Triassic Skagerrak data sets indicates under-compaction in three Central Graben samples sets (Judy, Heron and Skua) and significant chemical compaction in the Cod sample set (Table 5 & Figure 8). The low mechanical compaction state (under-compaction) of the Judy, Heron and Skua fields is further supported by petrographic evidence, such as floating grains and the frequency of low mechanical compaction grain contacts. The under-compaction in overpressured sandstones is likely result due to retardation of early mechanical compaction by overpressure development during shallow burial (<2500 m) (Bloch et al., 2002; Paxton et al., 2002). Overpressure, developed at shallow depth and continuously increased with ongoing burial, reduces the VES accrual and often leads to under-compaction, in relation to hydrostatically pressured sandstones at equivalent burial depth (e.g. Sclater and Christie, 1980), due to lower maximum VES acting on the grain framework. This can be observed in the Judy field, where IGV values are higher than expected (>26%, Table 5), due to shallow overpressure development and a constantly reduced VES accrual rate (Figure 7), resulting in the experience of lower maximum VES and a low mechanical compaction state for the present-day burial depth (e.g. Nguyen et al., 2013; Stricker and Jones, 2016). A similar correlation can be made for the present-day IGV values and the experienced maximum VES of the Heron and Skua fields, where IGV values are slightly higher than the expected 26% (Table 5 & Figure 8). The Cod sample set, demonstrated evidence for a high compaction state due to pressure solution at grain-to-grain contacts and a lower average IGV of around 21% (Table 6). This is most likely caused by the normal VES development prior to the deep overpressure onset (>2200 m), with a slow increase rate, which results a higher VES accrual rate and higher experienced maximum VES (36 MPa) during the burial history. The relationship between IGV and maximum VES in the Skagerrak samples sets demonstrate mechanical compaction is the main reservoir quality controlling factor, where measured IGV represents a good proxy (Figure 8).

VES development and influence on reservoir quality

Mechanical compaction, driven by VES, is recognised as an important porosity reducing process during shallow burial (0–2500 m) of siliciclastic sediments (Houseknecht, 1987, 1988; Paxton et al., 2002). Limiting the accrual rate or reducing the VES by overpressure during burial can slow down or arrest mechanical compaction and reduce its effect on porosity loss, leading to the maintenance of primary porosity to depth. This has been the subject of several empirical studies (e.g. Ramm and Bjørlykke, 1994; Gluyas and Cade, 1997) where the present-day porosities been related to present-day pore fluid overpressures. Hence the effect of overpressure development (i.e. timing, increase rate and maintenance) was not considered. However, the interaction of overpressure and the VES throughout the burial history must be considered to predict porosity preservation based on low mechanical compaction. Late development of overpressure at greater depth (for example by fluid transfer or expansion) will not be associated with a reduced compaction state. We infer that compaction has taken place by stress-sensitive porosity loss, both as mechanical compaction (i.e., grain rearrangement) and chemical compaction (i.e., pressure solution and cementation). The present-day compaction state of the sandstones has been determined by IGV measurements and the frequency measurements of distinctive petrographic features (i.e., grain contact types) in the fine-grained sandstones (Figure 9 & Table 6).

The importance of the VES development for the porosity preservation is highlighted by the comparison of two endmembers of this study; Judy and Cod. Even though both selected sample sets show the same primary attributes controlled by deposition (fine grained, well sorted, similar composition), they exhibit different present-day compaction states, reflecting different VES histories. The development of VES in the Joanne Sandstone Member of the Judy Field occurred from 90 Ma onwards. The rate of VES increase was arrested with early onset of overpressure at depth of 1350 m (Figure 7). The shallow overpressure development in the Joanne Sandstone Member reduced the VES accrual from

an early stage onwards, which led to a reduced maximum VES acting on the grain framework. This VES evolution is reflected by anomalously high present-day porosities (Figure 4), high average IGV values (Figure 8) and a high frequency of point contacts (Table 6 & Figure 9) in the Judy sample set. The higher present-day compaction state of the Cod sandstone samples on the other hand, reflects a more normal VES development of the Skagerrak Formation in the Cod field (Figure 7). VES in the sands started to increase slowly at around 150 Ma, with a significant increase of the VES accrual at 100 Ma, which was coupled to increased burial rate. VES increased to around 20 MPa prior to the main phase of overpressure development at a burial depth of ~2200 m (Figure 7). The development of VES to a burial depth of ~2200m led to the significant mechanical compaction and porosity loss of the Skagerrak Formation channel sands in the Cod field. The Cod field sample data set supports the burial and pressure modelling where low porosities (Figure 4), low average IGV (Table 5) and high frequencies of concavo-convex and sutured grain contact types, indicate a higher degree of compaction and pressure solution (Figure 9).

The comparison of the Judy and Cod sample sets shows that the compaction state and reservoir quality in the Skagerrak Formation sandstones in the North Sea are highly dependent on the experienced maximum VES, which has been controlled by the interplay of burial depth (i.e., stress induced by the overburden) and the pore fluid overpressure (Figure 9). The positive effect of overpressure or low VES towards retardation of mechanical compaction has been previously observed by modelling studies of (Lander and Walderhaug, 1999; Paxton et al., 2002). Furthermore, high primary porosities, maintained by shallow overpressure have been documented for the Skagerrak Formation sands of the Judy Field (Nguyen et al., 2013; Stricker and Jones 2016).

However, a recent study by Taylor et al. (2015) partly focusing on the Skagerrak Formation (Egret, Heron, Seagull & Skua) deny the contribution of shallow overpressure development and reduced VES towards the excellent reservoir quality in the UK Quadrant 22 and attribute the enhanced porosity to chlorite grain coatings. The role played by chlorite coatings in these reservoirs are significant in reducing quartz cementation and correlates

with quantities of quartz cement, but does not reflect the present-day compaction state, the high IGV values and low frequency of concavo-convex and sutured grain contacts in this region. We propose a mixed approach of low maximum VES and high fraction of chlorite coated grains for the porosity preservation in the Heron and Skua fields.

The petrographically observed results of this study complement the empirical porosity and VES trends discussed by (Grant et al., 2014). They looked at trends in total porosity within the Skagerrak Formation derived from petrophysical log analysis using V_{shale} and thickness filters to remove facies and bed-scale variability. These trends strongly suggested that compaction is the dominant factor controlling average reservoir porosity. The modelling done here, in conjunction with the petrographic observations help substantiate this model and provide petrographic evidence for the processes involved. Even at the grain scale the compaction state shows a correlation to the modelled estimated maximum VES during burial. Maximum VES typically occurred around 10 Ma before late burial and fluid pressure inflation.

When looked at carefully it is clear that other influences, beside VES can a role in determining reservoir quality. Chlorite coatings and the presence of microquartz rims (e.g. Taylor et al., 2015) dictate the ability of authigenic quartz cements to form at detrital grain surfaces and potentially occlude porosity. Low VES due to overpressure development helps retard pressure solution and thus restrict the amount of locally sourced silica available to enter into solution. In the absence of significant cementation, compaction is left to play its over-arching role.

Conclusion

- 1) Excellent reservoir quality with anomalously high porosity is preserved in many HPHT reservoirs of the Skagerrak Formation in the Central Graben, North Sea. However, despite similar diagenetic histories, reservoir quality and preserved porosity can vary from excellent to non-economic in HPHT reservoirs of the Central Graben area.
- 2) Excellent reservoir quality with anomalously high porosities of up to 35% at burial depth of >3500 m bsf is preserved in the UK sectors of the Central Graben. Shallow onset and continuous increase of overpressure reduced the VES in the Heron, Jade, Judy and Skua fields and resulted in under-compaction of the fluvial channel reservoirs for their present-day depth of burial.
- 3) Continuous compaction in the Norwegian HPHT reservoir sandstones (Cod & Gaupe) of the Central Graben reduced the reservoir quality with porosities <10% due to deeper overpressure onset and late VES reduction.
- 4) This research has demonstrated the importance of identifying the timing of overpressure generation and its maintenance for arresting mechanical compaction during progressive burial. The results are consistent with a model where VES affects both the compaction state and subsequent cementation of the reservoir. It has clearly identified the importance of VES in reservoir quality studies especially for HPHT basins.

Acknowledgments

The research consortium GeoPOP sponsored by BG, BP, Chevron, ConocoPhillips, DONG Energy, E.ON, ENI, Petrobras, Petronas, Statoil, Total and Tullow Oil, at Durham University are thanked for funding this research. We acknowledge support from the BGS for access to core material from the Heron Cluster wells. The results presented have been improved through collaborative discussions with many colleagues including Neil Goulty, Andy Aplin, Jon Gluyas, Jamie Middleton, Neil Meadows and Sean O'Neill.

Figures

Figure 1 - Regional base Cretaceous unconformity two-way time (TWT) map of the Central Graben, North Sea, highlighting the location of the six investigated Skagerrak Formation fields.

Figure 2 - Regional stratigraphy of the Central Graben, North Sea

Figure 3 - Grain size distribution and porosity for the Heron (136 samples), Skua (32), Jade (20), Judy (85), Cod (39) and Gaupe (90) sample sets, with the average (point), maximum and minimum porosity per grain size

Figure 4 – Helium (grey) and optical porosity (black) distribution with depth (in true vertical depth below mean sealevel) for the Heron, Skua, Jade, Judy (diamonds: 30/7a-9; points: 30/7a-7, -8, -11Z, -P3 & 30/13-5), Cod and Gaupe sample sets, with optical porosity of fine grained samples in solid black, a regional Central North Sea porosity-depth relationship for hydrostatically pressured shaly sandstone (Sclater and Christie, 1980). Large black circles represent PetroMod calibration porosity of the respective Skagerrak Formation sandstone.

Figure 5 - Compactional (COPL) and cementational (CEPL) porosity loss for the Heron, Skua, Jade, Judy, Cod and Gaupe fine grained data sets with remaining sample porosity (dashed lines). COPL and CEPL calculated after Lundegard (1992).

Figure 6 - Micrographs of thin sections highlighting different compaction stages, A) Judy (30/7a-8; 3502 m bsf): grain framework with 24% optical porosity and 'floating' grains; B) Jade (30/2c-4; 4605 m bsf): sample with 14.5% optical porosity; C) Gaupe (6/3-1; 2886 m bsf): densely packed grain framework with 7.5% optical porosity; D) Gaupe (6/3-1; 2885 m

bsf): bended and compressed mica grain; E) Cod (7/11-7; 4284 m bsf): concavo-convex grain contact; F) Cod (7/11-7; 4289 m bsf): sutured grain contact

Figure 7 - Evolution of burial depth (grey), pore fluid overpressure (OP) and vertical effective stress (VES) for the top of the Heron (22/29-5RES1), Skua (22/24b-7), Jade (30/2c-4), Judy (30/7a-9), Cod (7/11-7) and Gaupe (6/3-1) Skagerrak sandstone reservoirs

Figure 8 – Measured intergranular volumes, with average values, of Heron, Skua, Jade, Judy, Cod and Gaupe fine grained samples plotted against formational maximum vertical effective stress (VES) with a best fit trend lines for average IGV

Figure 9 - Fraction of point and concavo-convex grain contacts of Heron, Skua, Jade, Judy, Cod and Gaupe fine grained samples plotted against formational maximum vertical effective stress (VES) with best fit trend lines for average fraction point and concavo-convex contacts

Tables

Table 1 - Lithology type and respective thickness of the modelled layers for the Heron, Skua, Jade and Judy PetroMod models (the modelled key Skagerrak Formation reservoir unit in bold), with Sh: Shale, Sst: Sandstone, Non-Res.: Non-Reservoir Chalk and Res. Sst.: Reservoir Sandstone (80% Sand, 10% Silt and 10% Clay)

Table 2 - Lithology type and respective thickness of the modelled layers for the Cod and Gaupe models (the modelled key Skagerrak Formation reservoir unit in bold), with Sh: Shale and Res. Sst.: Reservoir Sandstone (80% Sand, 10% Silt and 10% Clay)

Table 3 - Non-reservoir North Sea Hod chalk model parameters, after Mallon and Swarbrick (2002, 2008)

Table 4 – Optical porosities categorised by grain size, helium porosities and average grain size per sample set.

Table 5 - Measured intergranular volume (IGV) of the Heron, Skua, Jade, Judy, Cod and Gaupe fine grained samples

Table 6 - Distribution of distinctive grain contacts (point contact, long or tangential contact, concavo-convex (C&C) contact, sutured contact) for selected fine grained samples of the Heron, Skua, Jade, Judy, Cod and Gaupe sample sets

Literature

- Allen, P.A., Allen, J.R., 1990. Basin analysis: principles and applications. Blackwell, Oxford.
- Andrews-Speed, C., Oxburgh, E.R., Cooper, B., 1984. Temperatures and depth-dependent heat flow in western North Sea. AAPG Bulletin, 68, 1764-1781.
- Beard, D., Weyl, P., 1973. Influence of Texture on Porosity and Permeability of unconsolidated Sand. AAPG Bulletin, 57, 349-369.
- Bishop, D.J., 1996. Regional distribution and geometry of salt diapirs and supra-Zechstein Group faults in the western and central North Sea. Marine and petroleum geology 13, 355-364.
- Bloch, S., Lander, R.H., Bonnell, L., 2002. Anomalous high porosity and permeability in deeply buried sandstone reservoirs: Origin and predictability. AAPG Bulletin 86, 301-328.
- Chuhan, F.A., Kjeldstad, A., Bjørlykke, K., Høeg, K., 2002. Porosity loss in sand by grain crushing—Experimental evidence and relevance to reservoir quality. Marine and Petroleum Geology, 19, 39-53.
- De Jong, M., Smith, D., Nio, S., Hardy, N., 2006. Subsurface correlation of the Triassic of the UK southern Central Graben: new look at an old problem. First Break, 24, 103-109.
- Ehrenberg, S., 1995. Measuring sandstone compaction from modal analysis of thin sections: how to do it and what the results mean. Journal of Sedimentary Research, 65, 369-379
- Erratt, D., Thomas, G., Wall, G., 1999. The evolution of the central North Sea Rift, Petroleum Geology of Northwest Europe: Proceedings of the 5th Conference. Geological Society, London, pp. 63-82.
- Glennie, K.W., 1998. Petroleum geology of the North Sea: basic concepts and recent advances. Blackwell, Oxford..
- Gluyas, J., Cade, C.A., 1997. Prediction of porosity in compacted sands. AAPG Memoir 69, 19-28.
- Goldsmith, P., Hudson, G., Van Veen, P., 2003. Triassic. The Millenium Atlas: Petroleum geology of the central and northern North Sea: Geological Society (London), 105-127
- Goldsmith, P., Rich, B., Standring, J., 1995. Triassic correlation and stratigraphy in the south Central Graben, UK North Sea. Geological Society, London, Special Publications 91, 123-143.
- Gowers, M.B., Sæbøe, A., 1985. On the structural evolution of the Central Trough in the Norwegian and Danish sectors of the North Sea. Marine and Petroleum Geology 2, 298-318.
- Grant, N.T., Middleton, A.J., Archer, S., 2014. Porosity trends in the Skagerrak Formation, Central Graben, United Kingdom Continental Shelf: The role of compaction and pore pressure history. AAPG Bulletin 98, 1111-1143.

- Grove, C., Jerram, D.A., 2011. jPOR: An ImageJ macro to quantify total optical porosity from blue-stained thin sections. *Computers & Geosciences* 37, 1850-1859.
- Houseknecht, D.W., 1984. Influence of grain size and temperature on intergranular pressure solution, quartz cementation, and porosity in a quartzose sandstone. *Journal of Sedimentary Research* 54, 348-361.
- Houseknecht, D.W., 1987. Assessing the Relative Importance of Compaction Processes and Cementation to Reduction of Porosity in Sandstones. *AAPG Bulletin* 71, 633-642.
- Houseknecht, D.W., 1988. Intergranular pressure solution in four quartzose sandstones. *Journal of Sedimentary Research* 58, 228-246.
- Isaksen, G.H., 2004. Central North Sea hydrocarbon systems: Generation, migration, entrapment, and thermal degradation of oil and gas. *AAPG Bulletin* 88, 1545-1572.
- Kape, S., De Souza, O.D., Bushnaq, I., Hayes, M., Turner, I., 2010. Predicting production behaviour from deep HPHT Triassic reservoirs and the impact of sedimentary architecture on recovery, Geological Society, London, Petroleum Geology Conference series. Geological Society of London, pp. 405-417.
- Lander, R.H., Walderhaug, O., 1999. Predicting porosity through simulating sandstone compaction and quartz cementation. *AAPG Bulletin* 83, 433-449.
- Lundegard, P.D., 1992. Sandstone porosity loss; a "big picture" view of the importance of compaction. *Journal of Sedimentary Petrology* 62, 250-260.
- Mallon, A., Swarbrick, R., 2002. A compaction trend for non-reservoir North Sea Chalk. *Marine and Petroleum Geology* 19, 527-539.
- Mallon, A., Swarbrick, R., 2008. Diagenetic characteristics of low permeability, non-reservoir chalks from the Central North Sea. *Marine and Petroleum Geology* 25, 1097-1108.
- Matthews, W.J., Hampson, G.J., Trudgill, B.D., Underhill, J.R., 2007. Controls on fluviolacustrine reservoir distribution and architecture in passive salt-diapir provinces: Insights from outcrop analogs. *AAPG Bulletin* 91, 1367-1403.
- McBride, E.F., 1989. Quartz cement in sandstones: a review. *Earth-Science Reviews* 26, 69-112.
- McKie, T., Audretsch, P., 2005. Depositional and structural controls on Triassic reservoir performance in the Heron Cluster, ETAP, Central North Sea, Geological Society, London, Petroleum Geology Conference series. Geological Society of London, pp. 285-297.
- Nguyen, B.T.T., Jones, S.J., Goult, N.R., Middleton, A.J., Grant, N., Ferguson, A., Bowen, L., 2013. The role of fluid pressure and diagenetic cements for porosity preservation in Triassic fluvial reservoirs of the Central Graben, North Sea. *AAPG Bulletin* 97, 1273-1302.
- Osborne, M.J., Swarbrick, R.E., 1997. Mechanisms for generating overpressure in sedimentary basins: A reevaluation. *AAPG Bulletin* 81, 1023-1041.

- Osborne, M.J., Swarbrick, R.E., 1999. Diagenesis in North Sea HPHT clastic reservoirs—Consequences for porosity and overpressure prediction. *Marine and Petroleum Geology* 16, 337-353.
- Paxton, S., Szabo, J., Ajdukiewicz, J., Klimentidis, R., 2002. Construction of an intergranular volume compaction curve for evaluating and predicting compaction and porosity loss in rigid-grain sandstone reservoirs. *AAPG Bulletin* 86, 2047-2067.
- Ramm, M., Bjørlykke, K., 1994. Porosity/depth trends in reservoir sandstones: Assessing the quantitative effects of varying pore-pressure, temperature history and mineralogy, Norwegian Shelf data. *Clay Minerals* 29, 475-490.
- Sclater, J.G., Christie, P.A.F., 1980. Continental stretching: An explanation of the post-Mid-Cretaceous subsidence of the central North Sea Basin. *Journal of Geophysical Research: Solid Earth* (1978–2012) 85, 3711-3739.
- Smith, R., Hodgson, N., Fulton, M., 1993. Salt control on Triassic reservoir distribution, UKCS central North Sea, Geological Society, London, Petroleum Geology Conference series. Geological Society of London, pp. 547-557.
- Stricker, S., Jones, S J., 2016. Enhanced porosity preservation by pore fluid overpressure and chlorite grain coatings in the Triassic Skagerrak, Central Graben, North Sea, UK. Geological Society, London, Special Publications, 435, doi:10.1144/SP435.4
- Swarbrick, R., Osborne, M., Grunberger, D., Yardley, G., Macleod, G., Aplin, A., Larter, S., Knight, I., Auld, H., 2000. Integrated study of the Judy field (Block 30/7a)—An overpressured central North Sea oil/gas field. *Marine and Petroleum Geology* 17, 993-1010.
- Swarbrick, R.E., Lahann, R.W., O'Connor, S.A., Mallon, A.J., 2010. Role of the Chalk in development of deep overpressure in the Central North Sea, Geological Society, London, Petroleum Geology Conference series. Geological Society of London, pp. 493-507.
- Swarbrick, R.E., Osborne, M.J., 1998. Mechanisms that Generate Abnormal Pressures: an Overview. *AAPG Memoir* 70, 13-34
- Swarbrick, R.E., Osborne, M.J., Yardley, G.S., 2002. Comparison of overpressure magnitude resulting from the main generating mechanisms. *AAPG Memoir* 76, 1-12.
- Taylor, T.R., Giles, M.R., Hathon, L.A., Diggs, T.N., Braunsdorf, N.R., Birbiglia, G.V., Kittridge, M.G., Macaulay, C.I., Espejo, I.S., 2010. Sandstone diagenesis and reservoir quality prediction: Models, myths, and reality. *AAPG Bulletin* 94, 1093-1132.
- Taylor, T.R., Kittridge, M.G., Winefield, P., Bryndzia, L.T., Bonnell, L.M., 2015. Reservoir quality and rock properties modeling—Triassic and Jurassic sandstones, greater Shearwater area, UK Central North Sea. *Marine and Petroleum Geology* 65, 1-21.
- Vagle, G.B., Hurst, A., Dypvik, H., 1994. Origin of quartz cements in some sandstones from the Jurassic of the Inner Moray Firth (UK). *Sedimentology* 41, 363-377.
- Walderhaug, O., 1990. A Fluid Inclusion Study of Quartz-Cemented Sandstones from Offshore Mid-Norway--Possible Evidence for Continued Quartz Cementation During Oil Emplacement. *Journal of Sedimentary Research* 60, 203-210.

Walderhaug, O., 1994. Precipitation rates for quartz cement in sandstones determined by fluid-inclusion microthermometry and temperature-history modeling. *Journal of Sedimentary Research* 64, 311-323.

Worden, R., Morad, S., 2000. Quartz cementation in oilfield sandstones: a review of the key controversies. *Special Publication, International Association of Sedimentologists*, 1-20.

Group/ Formation	Heron (22/29-5RE)		Skua (22/24b-7)		Jade (30/2c-4)		Judy (30/7a-9)	
	Thick.	Lithology	Thick.	Lithology	Thick.	Lithology	Thick.	Lithology
	[m]	[-]	[m]	[-]	[m]	[-]	[m]	[-]
Nordland	1407	Shale	1762	Shale	1624	Shale	1424	Shale
Lark/Horda	1396	Shale	957	Shale	1364	Shale	1357	Shale
Tay	15	Sandy Sh.						
Balder	18	Shale	12	Shale	22	Silty Sh.	17	Silty Sh.
Sele	31	Sandy Sh.	21	Shale	39	Silty Sh.	54	Silty Sh.
Forties	187	Sandstone	79	Sandstone	58	Sandstone		
Lista	49	Silty Sh.			16	Shale	16	Shale
Mey					24	Shale		
Andrew	51	Siltstone	81	Siltstone			89	Silty Sh.
Maureen	82	Marl	54	Marl	135	Sandstone	92	Sst/Marl
Ekofisk	94	Chalk	76	Marl	83	Marl	28	Chalk
Tor	459	Chalk	300	Chalk	506	Marl	226	Chalk
Hod	335	Non-Res.	98	Non-Res.	529	Non-Res.	154	Non-Res.
Herring	9	Marl						
Valhall	63	Marl	19	Marl	87	Shale	22	Sandy Sh.
Humber	0	Shale	0	Shale	0	Shale	0	Shale
Lias							3	Shale
Fladen	0	Sandstone	0	Sandstone	0	Sandstone	0	Sandstone
Joshua	0	Silty Shale	0	Silty Sh.	0	Silty Sh.	0	Silty Sh.
Josephine	0	Res. Sst	0	Res. Sst	0	Res. Sst	0	Res. Sst
Jonathan	0	Silty Sh.	0	Silty Sh.	0	Silty Sh.	38	Silty Sh.
Joanne	23	Res. Sst	0	Res. Sst	384	Res. Sst	469	Res. Sst
Julius	41	Silty Sh.	0	Silty Sh.	54	Silty Sh.	140	Silty Sh.
Judy	339	Res. Sst	468	Res. Sst	400	Res. Sst	385	Res. Sst
Smith Bank	200	Silty Sh.	118	Silty Sh.	600	Silty Sh.	200	Silty Sh.
Zechstein	208	Salt	207	Salt	500	Salt	208	Salt

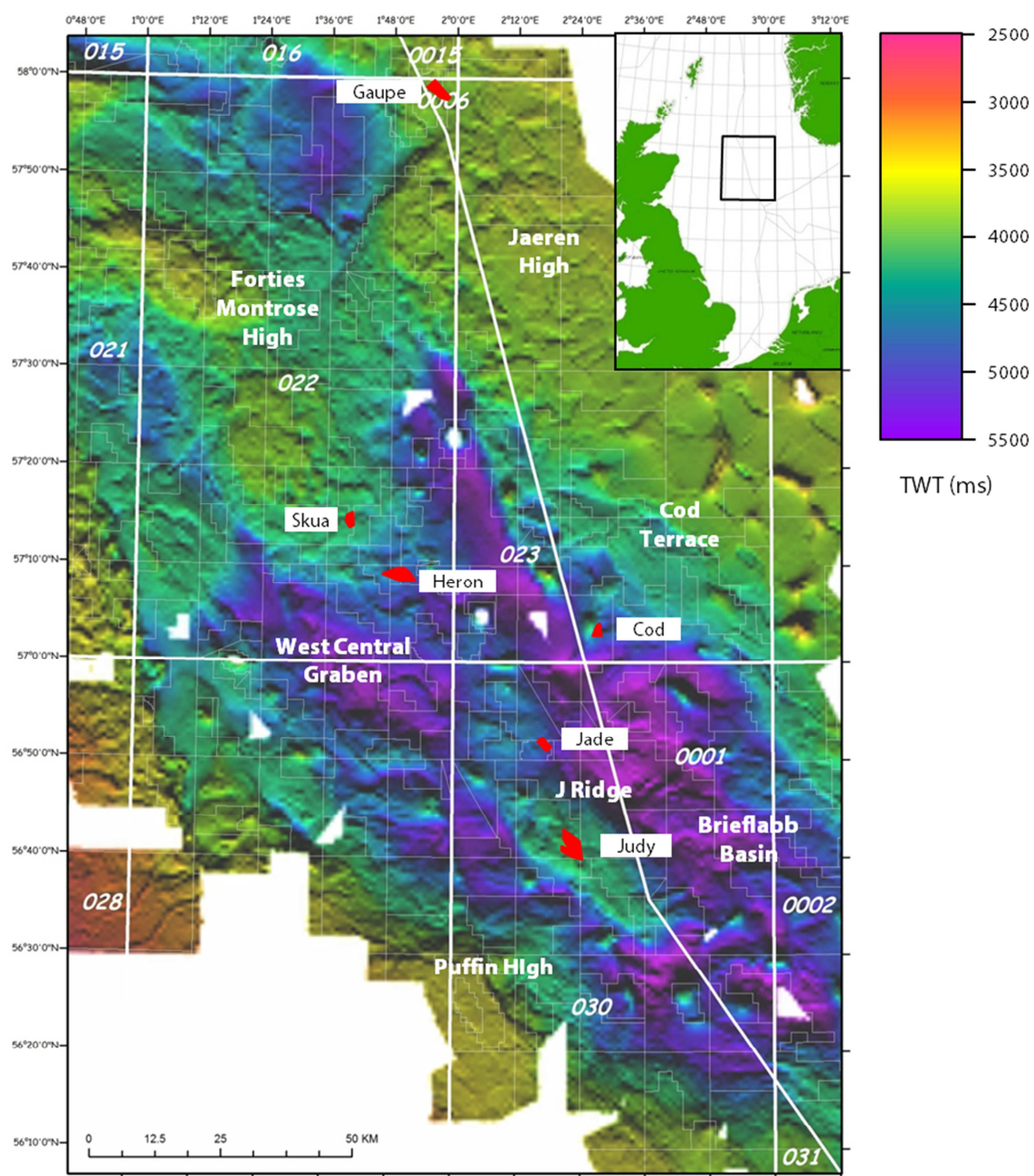
Group/ Formation	Cod (7/11-7)		Gaupe (6/3-1)	
	Thick.	Lithology	Thick.	Lithology
	[m]	[-]	[m]	[-]
Nordland	1503	Shale	1211	Shale
Hordaland	1317	Shale	1115	Shale
Balder	13	Shale	14	Shale
Sele	39	Shale	87	Shale
Lista	190	Sandy Sh.	1	Shale
Maureen	13	Sandy Sh.	136	Chalk
Ekofisk	79	Chalk	6	Chalk
Tor	405	Chalk	165	Chalk
Hod	324	Chalk	78	Chalk
Blodoks	8	Shale		
Hidra	109	Chalk		
Rodby	41	Marl		
Asgard	42	Marl	41	Shale
Mandal	42	Shale		
Farsund	78	Shale	2	Shale
Ula	38	Sandstone		
Gassum			13	Sandstone
Skagerrak	287	Res. Sst	545	Res. Sst
Smith Bank	200	Silty Sh.	200	Silty Sh.
Zechstein	200	Salt	200	Salt

Model Parameter (Hod Formation)			
Mechanical compaction		Permeability	
Porosity	Depth	Porosity	Permeability
[%]	[m]	[%]	[log(mD)]
70.00	0	70.00	1.00
18.00	1300	30.00	-1.00
12.50	2100	25.00	-3.00
8.00	3100	20.00	-5.50
5.00	4500	12.50	-7.20
		9.00	-7.20
		5.00	-7.20

Field	Porosity	Optical porosity by grain size					Helium porosity	Average grain size
		Silt	Sand					
		Silt	very fine	fine	medium	coarse		
		[mm]	[mm]	[mm]	[mm]	[mm]		
Heron	Maximum	3.9	12.9	24.5	30.9		29	0.136
	Average	1.8	3.2	7.6	18		19.5	
	Minimum	0.4	1	0.9	5.4		2.1	
Skua	Maximum		14.4	32.2			27.8	0.169
	Average		10.4	11			17.4	
	Minimum		6.5	3.1			2.2	
Jade	Maximum		12.3	17.5			26.2	0.146
	Average		2.2	11	16.8		15.8	
	Minimum		0.3	0.7			3.7	
Judy	Maximum	2	18.3	28.1			35.6	0.145
	Average	0.9	6.4	16.1	25.7		23.3	
	Minimum	0.3	0.2	0.3			2.3	
Cod	Maximum		5.9	10.3	6.5		20.4	0.204
	Average	0.6	3.1	3.9	3.9		9.8	
	Minimum		0.6	0.3	0.1		1.8	
Gaupe	Maximum		6.1	17.8	25.1	20.4	24.9	0.323
	Average		5.4	4.9	10.4	11.1	14.3	
	Minimum		4.9	0.2	1.5	0.6	1.9	

Field	IGV		
	Minimum	Average	Maximum
Heron	20	27.3	36
Skua	19	27.1	34.3
Jade	15	22.2	28
Judy	19.33	28.2	36.3
Cod	15	21.1	34
Gaupe	9.3	25.7	35

Sample data			Grain contacts [%]			
Field	Well	Sample	Point	Long	C&C	Sutured
Heron	22 29-5RE	15614'9	16.00	52.00	32.00	0.00
		15675'10	12.00	48.00	40.00	0.00
		15691'6	18.00	46.00	36.00	0.00
		15724'11	16.00	46.00	38.00	0.00
		15749'1	22.00	36.00	42.00	0.00
		15760'11	14.00	46.00	40.00	0.00
		Average	16.33	45.67	38.00	0.00
Skua	22 24b-7	11909'4	8.00	42.00	44.00	6.00
		11932'	4.00	50.00	42.00	4.00
		11882'2	12.00	42.00	46.00	0.00
		12086'3	18.00	44.00	38.00	0.00
		11971'1	16.00	40.00	42.00	2.00
		11908'3	10.00	44.00	44.00	2.00
		Average	11.33	43.67	42.67	2.33
Jade	30 2c-4	s8 - 15615.94	10.00	52.00	34.00	4.00
		15645	22.00	46.00	32.00	0.00
		15660	14.00	44.00	36.00	6.00
		s11 - 15660.33	8.00	46.00	46.00	0.00
		15678	20.00	36.00	40.00	4.00
		15748	16.00	32.00	50.00	2.00
		Average	15.00	42.67	39.67	2.67
Judy	30 7a-7	11496	24.00	46.00	30.00	0.00
	30 7a-8	11688	32.00	46.00	22.00	0.00
		11731	32.00	46.00	22.00	0.00
		11820	44.00	34.00	22.00	0.00
	30 7a-9	12077	34.00	42.00	24.00	0.00
		12167	30.00	46.00	24.00	0.00
	30 7a-11Z	s12 - 11438.98	36.00	44.00	20.00	0.00
		s42 - 11660.53	32.00	42.00	26.00	0.00
		Average	33.00	43.25	23.75	0.00
Cod	7 11-7	4614.06	0.00	20.00	70.00	10.00
		4606.44	6.00	32.00	60.00	2.00
		4594.86	6.00	24.00	60.00	10.00
		4609.19	2.00	32.00	56.00	10.00
		4616.2	0.00	24.00	60.00	16.00
		Average	2.80	26.40	61.20	9.60
Gaupe	6 3-1	3063	8.00	48.00	42.00	2.00
		3102.03	10.00	34.00	52.00	4.00
		3107.77	12.00	42.00	44.00	2.00
		3108.75	4.00	42.00	46.00	8.00
		3061.1	6.00	48.00	44.00	2.00
		Average	8.00	42.80	45.60	3.60



Tectonics	Epoch		United Kingdom		Lithology	Norway		Lithology	Key	
	Series		Group Formation			Group Formation				
Postrift	Quaternary		Nordland			Nordland	Naust			
	Neogene	Pli.	Westray	Lark		Westray	Lark			Shale
		Miocene								
	Paleogene	Oli.	Stronsay	Horda		Stronsay	Horda			Sandstone
			Moray	Balder			Balder			
		Paleocene		Sele		Moray	Sele			Chalk
			Montrose	Lista		Montrose	Lista			
		Maureen			Vale					
	Cretaceous		Upper	Chalk	Ekofisk		Shetland	Ekofisk		
		Tor			Tor					
		Hod			Hod					
		Herring			Blodoks					
		Hidra			Hidra					
		Lower	Cromer Knoll	Rodby		Cromer Knoll	Rodby		Volcanics	
	Valhall	Asgard								
Synrift	Jurassic	Upper	Humber	Kimmeridge Clay		Tyne	Mandal		V	
Heather							Farsund			
Postrift		Mid	Fladen	Pentland		Vestland	Ula		Unconformity	
	Triassic	Upper	Skagerrak		Hegre	Skagerrak				
Synrift		Lower		Smith Bank			Smith Bank			
Postrift	Permian		Zechstein	Shearwater		Zechstein	Shearwater			
Synrift			Rotliegendes	Auk		Rotliegendes	Auk			
	Devonian	Up	Old Red	Buchan		Old Red	Buchan			

